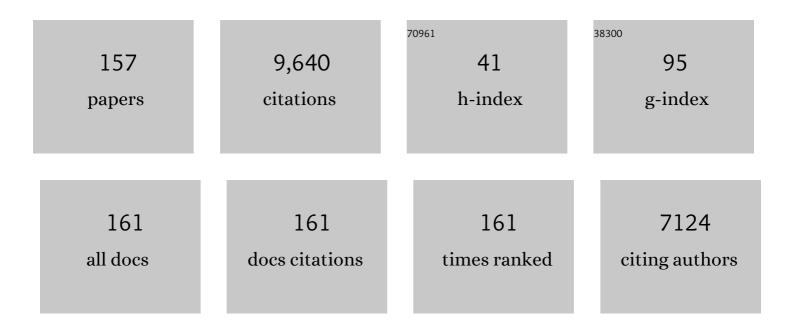
Grzegorz Greczynski

List of Publications by Year in descending order

Source: https://exaly.com/author-pdf/4740573/publications.pdf Version: 2024-02-01



#	Article	IF	CITATIONS
1	X-ray photoelectron spectroscopy: Towards reliable binding energy referencing. Progress in Materials Science, 2020, 107, 100591.	16.0	1,284
2	Reliable determination of chemical state in x-ray photoelectron spectroscopy based on sample-work-function referencing to adventitious carbon: Resolving the myth of apparent constant binding energy of the C 1s peak. Applied Surface Science, 2018, 451, 99-103.	3.1	821
3	The effects of solvents on the morphology and sheet resistance in poly(3,4-ethylenedioxythiophene)–polystyrenesulfonic acid (PEDOT–PSS) films. Synthetic Metals, 2003, 139, 1-10.	2.1	702
4	C 1s Peak of Adventitious Carbon Aligns to the Vacuum Level: Dire Consequences for Material's Bonding Assignment by Photoelectron Spectroscopy. ChemPhysChem, 2017, 18, 1507-1512.	1.0	695
5	Compromising Science by Ignorant Instrument Calibration—Need to Revisit Half a Century of Published XPS Data. Angewandte Chemie - International Edition, 2020, 59, 5002-5006.	7.2	429
6	Characterization of the PEDOT-PSS system by means of X-ray and ultraviolet photoelectron spectroscopy. Thin Solid Films, 1999, 354, 129-135.	0.8	390
7	Photoelectron spectroscopy of thin films of PEDOT–PSS conjugated polymer blend: a mini-review and some new results. Journal of Electron Spectroscopy and Related Phenomena, 2001, 121, 1-17.	0.8	389
8	The same chemical state of carbon gives rise to two peaks in X-ray photoelectron spectroscopy. Scientific Reports, 2021, 11, 11195.	1.6	353
9	Compromising Science by Ignorant Instrument Calibration—Need to Revisit Half a Century of Published XPS Data. Angewandte Chemie, 2020, 132, 5034-5038.	1.6	143
10	A step-by-step guide to perform x-ray photoelectron spectroscopy. Journal of Applied Physics, 2022, 132,	1.1	141
11	Self-consistent modelling of X-ray photoelectron spectra from air-exposed polycrystalline TiN thin films. Applied Surface Science, 2016, 387, 294-300.	3.1	131
12	A review of metal-ion-flux-controlled growth of metastable TiAlN by HIPIMS/DCMS co-sputtering. Surface and Coatings Technology, 2014, 257, 15-25.	2.2	126
13	Role of Tin+ and Aln+ ion irradiation (n=1, 2) during Ti1-xAlxN alloy film growth in a hybrid HIPIMS/magnetron mode. Surface and Coatings Technology, 2012, 206, 4202-4211.	2.2	119
14	Time and energy resolved ion mass spectroscopy studies of the ion flux during high power pulsed magnetron sputtering of Cr in Ar and Ar/N2 atmospheres. Vacuum, 2010, 84, 1159-1170.	1.6	116
15	XPS guide: Charge neutralization and binding energy referencing for insulating samples. Journal of Vacuum Science and Technology A: Vacuum, Surfaces and Films, 2020, 38, .	0.9	114
16	Towards reliable X-ray photoelectron spectroscopy: Sputter-damage effects in transition metal borides, carbides, nitrides, and oxides. Applied Surface Science, 2021, 542, 148599.	3.1	110
17	Core-level spectra and binding energies of transition metal nitrides by non-destructive x-ray photoelectron spectroscopy through capping layers. Applied Surface Science, 2017, 396, 347-358.	3.1	109
18	Metal versus rare-gas ion irradiation during Ti1â^' <i>x</i> Al <i>x</i> N film growth by hybrid high power pulsed magnetron/dc magnetron co-sputtering using synchronized pulsed substrate bias. Journal of Vacuum Science and Technology A: Vacuum, Surfaces and Films, 2012, 30, .	0.9	98

#	Article	IF	CITATIONS
19	Paradigm shift in thin-film growth by magnetron sputtering: From gas-ion to metal-ion irradiation of the growing film. Journal of Vacuum Science and Technology A: Vacuum, Surfaces and Films, 2019, 37, .	0.9	94
20	Venting temperature determines surface chemistry of magnetron sputtered TiN films. Applied Physics Letters, 2016, 108, .	1.5	92
21	An experimental study of poly(9,9-dioctyl-fluorene) and its interfaces with Li, Al, and LiF. Journal of Chemical Physics, 2000, 113, 2407-2412.	1.2	89
22	Functionalization of bacterial cellulose wound dressings with the antimicrobial peptide <i>ε</i> -poly-L-Lysine. Biomedical Materials (Bristol), 2018, 13, 025014.	1.7	86
23	The electronic structure of polymer–metal interfaces studied by ultraviolet photoelectron spectroscopy. Materials Science and Engineering Reports, 2001, 34, 121-146.	14.8	84
24	Microstructure control of CrNx films during high power impulse magnetron sputtering. Surface and Coatings Technology, 2010, 205, 118-130.	2.2	77
25	<pre>\$hbox{CrN}_{m x}\$ Films Prepared by DC Magnetron Sputtering and High-Power Pulsed Magnetron Sputtering: A Comparative Study. IEEE Transactions on Plasma Science, 2010, 38, 3046-3056.</pre>	0.6	72
26	Strain-free, single-phase metastable Ti0.38Al0.62N alloys with high hardness: metal-ion energy vs. momentum effects during film growth by hybrid high-power pulsed/dc magnetron cosputtering. Thin Solid Films, 2014, 556, 87-98.	0.8	69
27	Reference binding energies of transition metal carbides by core-level x-ray photoelectron spectroscopy free from Ar+ etching artefacts. Applied Surface Science, 2018, 436, 102-110.	3.1	68
28	Selection of metal ion irradiation for controlling Ti1â^'xAlxN alloy growth via hybrid HIPIMS/magnetron co-sputtering. Vacuum, 2012, 86, 1036-1040.	1.6	66
29	Structural and mechanical properties of Cr–Al–O–N thin films grown by cathodic arc deposition. Acta Materialia, 2012, 60, 6494-6507.	3.8	65
30	Improving the high-temperature oxidation resistance of TiB2 thin films by alloying with Al. Acta Materialia, 2020, 196, 677-689.	3.8	65
31	X-ray photoelectron spectroscopy studies of Ti1-Al N (0†â‰≇€ x†â‰≇€ 0.83) high-temperature oxidation: Th crucial role of Al concentration. Surface and Coatings Technology, 2019, 374, 923-934.	1e 2.2	64
32	Stability of 10B4C thin films under neutron radiation. Radiation Physics and Chemistry, 2015, 113, 14-19.	1.4	53
33	Control of Ti1â^'xSixN nanostructure via tunable metal-ion momentum transfer during HIPIMS/DCMS co-deposition. Surface and Coatings Technology, 2015, 280, 174-184.	2.2	53
34	Ti ₂ Au ₂ C and Ti ₃ Au ₂ C ₂ formed by solid state reaction of gold with Ti ₂ AlC and Ti ₃ AlC ₂ . Chemical Communications, 2017, 53, 9554-9557.	2.2	53
35	Peak amplitude of target current determines deposition rate loss during high power pulsed magnetron sputtering. Vacuum, 2016, 124, 1-4.	1.6	51
36	Mitigating the geometrical limitations of conventional sputtering by controlling the ion-to-neutral ratio during high power pulsed magnetron sputtering. Thin Solid Films, 2011, 519, 6354-6361.	0.8	48

#	Article	IF	CITATIONS
37	Controlling the B/Ti ratio of TiBx thin films grown by high-power impulse magnetron sputtering. Journal of Vacuum Science and Technology A: Vacuum, Surfaces and Films, 2018, 36, .	0.9	46
38	Novel strategy for low-temperature, high-rate growth of dense, hard, and stress-free refractory ceramic thin films. Journal of Vacuum Science and Technology A: Vacuum, Surfaces and Films, 2014, 32, .	0.9	45
39	CFx thin solid films deposited by high power impulse magnetron sputtering: Synthesis and characterization. Surface and Coatings Technology, 2011, 206, 646-653.	2.2	43
40	Strategy for simultaneously increasing both hardness and toughness in ZrB2-rich Zr1â^'xTaxBy thin films. Journal of Vacuum Science and Technology A: Vacuum, Surfaces and Films, 2019, 37, .	0.9	42
41	Nitrogen-doped bcc-Cr films: Combining ceramic hardness with metallic toughness and conductivity. Scripta Materialia, 2016, 122, 40-44.	2.6	41
42	Electronic structure of hybrid interfaces of poly(9,9-dioctylfluorene). Chemical Physics Letters, 2000, 321, 379-384.	1.2	40
43	Unprecedented Al supersaturation in single-phase rock salt structure VAIN films by Al+ subplantation. Journal of Applied Physics, 2017, 121, .	1.1	40
44	Controlling the boron-to-titanium ratio in magnetron-sputter-deposited TiBx thin films. Journal of Vacuum Science and Technology A: Vacuum, Surfaces and Films, 2017, 35, .	0.9	40
45	Joint Theoretical and Experimental Characterization of the Structural and Electronic Properties of Poly(dioctylfluorene-alt-N-butylphenyl diphenylamine). Journal of Physical Chemistry B, 2004, 108, 5594-5599.	1.2	38
46	Improved adhesion of carbon nitride coatings on steel substrates using metal HiPIMS pretreatments. Surface and Coatings Technology, 2016, 302, 454-462.	2.2	37
47	Microstructure and mechanical, electrical, and electrochemical properties of sputter-deposited multicomponent (TiNbZrTa)Nx coatings. Surface and Coatings Technology, 2020, 389, 125651.	2.2	37
48	lon mass spectrometry investigations of the discharge during reactive high power pulsed and direct current magnetron sputtering of carbon in Ar and Ar/N2. Journal of Applied Physics, 2012, 112, .	1.1	36
49	Strategy for tuning the average charge state of metal ions incident at the growing film during HIPIMS deposition. Vacuum, 2015, 116, 36-41.	1.6	34
50	Industrial-scale deposition of highly adherent CNx films on steel substrates. Surface and Coatings Technology, 2010, 204, 3349-3357.	2.2	33
51	Al capping layers for nondestructive x-ray photoelectron spectroscopy analyses of transition-metal nitride thin films. Journal of Vacuum Science and Technology A: Vacuum, Surfaces and Films, 2015, 33, .	0.9	33
52	Stoichiometric, epitaxial ZrB2 thin films with low oxygen-content deposited by magnetron sputtering from a compound target: Effects of deposition temperature and sputtering power. Journal of Crystal Growth, 2015, 430, 55-62.	0.7	33
53	Oxidation behaviour of V2AlC MAX phase coatings. Journal of the European Ceramic Society, 2020, 40, 4436-4444.	2.8	33
54	Hybrid interfaces of poly(9,9-dioctylfluorene) employing thin insulating layers of CsF: A photoelectron spectroscopy study. Journal of Chemical Physics, 2001, 114, 8628-8636.	1.2	32

#	Article	IF	CITATIONS
55	Time evolution of ion fluxes incident at the substrate plane during reactive high-power impulse magnetron sputtering of groups IVb and VIb transition metals in Ar/N2. Journal of Vacuum Science and Technology A: Vacuum, Surfaces and Films, 2018, 36, .	0.9	31
56	Effect of ion-implantation-induced defects and Mg dopants on the thermoelectric properties of ScN. Physical Review B, 2018, 98, .	1.1	31
57	Effect of impurities on morphology, growth mode, and thermoelectric properties of (1 1 1) and (0 C epitaxial-like ScN films. Journal Physics D: Applied Physics, 2019, 52, 035302.) 1) 1.3	31
58	Metal-ion subplantation: A game changer for controlling nanostructure and phase formation during film growth by physical vapor deposition. Journal of Applied Physics, 2020, 127, .	1.1	30
59	High Si content TiSiN films with superior oxidation resistance. Surface and Coatings Technology, 2020, 398, 126087.	2.2	30
60	Energy level alignment in organic-based three-layer structures studied by photoelectron spectroscopy. Journal of Applied Physics, 2000, 88, 7187-7191.	1.1	28
61	Effect of substrate temperature on properties of diamond-like films deposited by combined DC impulse vacuum-arc method. Surface and Coatings Technology, 2013, 236, 444-449.	2.2	28
62	Low-temperature growth of dense and hard Ti0.41Al0.51Ta0.08N films via hybrid HIPIMS/DC magnetron co-sputtering with synchronized metal-ion irradiation. Journal of Applied Physics, 2017, 121, .	1,1	28
63	Age hardening in superhard ZrB2-rich Zr1-xTaxBy thin films. Scripta Materialia, 2021, 191, 120-125.	2.6	28
64	Gas rarefaction effects during high power pulsed magnetron sputtering of groups IVb and VIb transition metals in Ar. Journal of Vacuum Science and Technology A: Vacuum, Surfaces and Films, 2017, 35, .	0.9	27
65	Polymer interfaces studied by photoelectron spectroscopy: Li on polydioctylfluorene and Alq3. Thin Solid Films, 2000, 363, 322-326.	0.8	26
66	<i>In-situ</i> observation of self-cleansing phenomena during ultra-high vacuum anneal of transition metal nitride thin films: Prospects for non-destructive photoelectron spectroscopy. Applied Physics Letters, 2016, 109, .	1.5	26
67	Systematic compositional analysis of sputter-deposited boron-containing thin films. Journal of Vacuum Science and Technology A: Vacuum, Surfaces and Films, 2021, 39, .	0.9	26
68	Electronic structure of poly(9,9-dioctylfluorene) in the pristine and reduced state. Journal of Chemical Physics, 2002, 116, 1700-1706.	1.2	25
69	Unintentional carbide formation evidenced during high-vacuum magnetron sputtering of transition metal nitride thin films. Applied Surface Science, 2016, 385, 356-359.	3.1	25
70	Enhanced Ti0.84Ta0.16N diffusion barriers, grown by a hybrid sputtering technique with no substrate heating, between Si(001) wafers and Cu overlayers. Scientific Reports, 2018, 8, 5360.	1.6	25
71	Control of the metal/gas ion ratio incident at the substrate plane during high-power impulse magnetron sputtering of transition metals in Ar. Thin Solid Films, 2017, 642, 36-40.	0.8	24
72	Improved oxidation properties from a reduced B content in sputter-deposited TiBx thin films. Surface and Coatings Technology, 2021, 420, 127353.	2.2	24

#	Article	IF	CITATIONS
73	V0.5Mo0.5Nx/MgO(001): Composition, nanostructure, and mechanical properties as a function of film growth temperature. Acta Materialia, 2017, 126, 194-201.	3.8	23
74	Toward energy-efficient physical vapor deposition: Routes for replacing substrate heating during magnetron sputter deposition by employing metal ion irradiation. Surface and Coatings Technology, 2021, 415, 127120.	2.2	23
75	Rolling performance of carbon nitride-coated bearing components in different lubrication regimes. Tribology International, 2017, 114, 141-151.	3.0	22
76	Influence of Si content on phase stability and mechanical properties of TiAlSiN films grown by AlSi-HiPIMS/Ti-DCMS co-sputtering. Surface and Coatings Technology, 2021, 427, 127661.	2.2	22
77	Rolling contact fatigue of bearing components coated with carbon nitride thin films. Tribology International, 2016, 98, 100-107.	3.0	21
78	Multifunctional ZrB2-rich Zr1-xCrxBy thin films with enhanced mechanical, oxidation, and corrosion properties. Vacuum, 2021, 185, 109990.	1.6	21
79	X-ray Photoelectron Spectroscopy Analyses of the Electronic Structure of Polycrystalline Ti1-xAlxN Thin Films with 0â€‰â‰æ€‰xâ€‰â‰æ€‰0.96. Surface Science Spectra, 2014, 21, 35-49.	0.3	20
80	A comparative study of direct current magnetron sputtering and high power impulse magnetron sputtering processes for CNx thin film growth with different inert gases. Diamond and Related Materials, 2016, 64, 13-26.	1.8	20
81	Chemical bonding in epitaxial ZrB2 studied by X-ray spectroscopy. Thin Solid Films, 2018, 649, 89-96.	0.8	20
82	Electronic structure of β-Ta films from X-ray photoelectron spectroscopy and first-principles calculations. Applied Surface Science, 2019, 470, 607-612.	3.1	20
83	Ti–Si–C–N thin films grown by reactive arc evaporation from Ti ₃ SiC ₂ cathodes. Journal of Materials Research, 2011, 26, 874-881.	1.2	19
84	Extended metastable Al solubility in cubic VAIN by metal-ion bombardment during pulsed magnetron sputtering: film stress <i>vs</i> subplantation. Journal of Applied Physics, 2017, 122, .	1.1	19
85	Highly Stable and Efficient Ligninâ€PEDOT/PSS Composites for Removal of Toxic Metals. Advanced Sustainable Systems, 2018, 2, 1700114.	2.7	19
86	Exploring NiO nanosize structures for ammonia sensing. Journal of Materials Science: Materials in Electronics, 2018, 29, 11870-11877.	1.1	19
87	Control over the Phase Formation in Metastable Transition Metal Nitride Thin Films by Tuning the Al+ Subplantation Depth. Coatings, 2019, 9, 17.	1.2	19
88	Influence of inert gases on the reactive high power pulsed magnetron sputtering process of carbon-nitride thin films. Journal of Vacuum Science and Technology A: Vacuum, Surfaces and Films, 2013, 31, .	0.9	18
89	Selectable phase formation in VAIN thin films by controlling Al+ subplantation depth. Scientific Reports, 2017, 7, 17544.	1.6	18
90	Reactive high power impulse magnetron sputtering of CFx thin films in mixed Ar/CF4 and Ar/C4F8 discharges. Thin Solid Films, 2013, 542, 21-30.	0.8	17

#	Article	IF	CITATIONS
91	Low-temperature growth of low friction wear-resistant amorphous carbon nitride thin films by mid-frequency, high power impulse, and direct current magnetron sputtering. Journal of Vacuum Science and Technology A: Vacuum, Surfaces and Films, 2015, 33, .	0.9	17
92	Morphology effects on electrocatalysis of anodic water splitting on nickel (II) oxide. Microporous and Mesoporous Materials, 2022, 333, 111734.	2.2	17
93	Oxidation kinetics of overstoichiometric TiB2 thin films grown by DC magnetron sputtering. Corrosion Science, 2022, 206, 110493.	3.0	17
94	An experimental study of poly(9,9-dioctyl-fluorene) and its interface with Li and LiF Applied Surface Science, 2000, 166, 380-386.	3.1	16
95	Influence of Ti–Si cathode grain size on the cathodic arc process and resulting Ti–Si–N coatings. Surface and Coatings Technology, 2013, 235, 637-647.	2.2	16
96	Novel transparent MgSiON thin films with high hardness and refractive index. Vacuum, 2016, 131, 1-4.	1.6	16
97	Synthesis and characterization of single-phase epitaxial Cr2N thin films by reactive magnetron sputtering. Journal of Materials Science, 2019, 54, 1434-1442.	1.7	16
98	Effect of nitrogen content on microstructure and corrosion resistance of sputter-deposited multicomponent (TiNbZrTa)Nx films. Surface and Coatings Technology, 2020, 404, 126485.	2.2	16
99	Impact of B_4C co-sputtering on structure and optical performance of Cr/Sc multilayer X-ray mirrors. Optics Express, 2017, 25, 18274.	1.7	15
100	Surface functionalization of epitaxial graphene using ion implantation for sensing and optical applications. Carbon, 2020, 157, 169-184.	5.4	15
101	Self-organized columnar Zr0.7Ta0.3B1.5 core/shell-nanostructure thin films. Surface and Coatings Technology, 2020, 401, 126237.	2.2	15
102	Towards energy-efficient physical vapor deposition: Mapping out the effects of W+ energy and concentration on the densification of TiAlWN thin films grown with no external heating. Surface and Coatings Technology, 2021, 424, 127639.	2.2	15
103	An experimental study of poly(9,9-dioctyl-fluorene) and its interfaces with Al, LiF and CsF. Applied Surface Science, 2001, 175-176, 319-325.	3.1	14
104	Theoretical and experimental study of metastable solid solutions and phase stability within the immiscible Ag-Mo binary system. Journal of Applied Physics, 2016, 119, .	1.1	14
105	TiN diffusion barrier failure by the formation of Cu3Si investigated by electron microscopy and atom probe tomography. Journal of Vacuum Science and Technology B:Nanotechnology and Microelectronics, 2016, 34, .	0.6	13
106	Growth of dense, hard yet low-stress Ti0.40Al0.27W0.33N nanocomposite films with rotating substrate and no external substrate heating. Journal of Vacuum Science and Technology A: Vacuum, Surfaces and Films, 2020, 38, .	0.9	13
107	ZrCuAlNi thin film metallic glass grown by high power impulse and direct current magnetron sputtering. Surface and Coatings Technology, 2021, 412, 127029.	2.2	13
108	Electronic structure of pristine and sodium doped poly(p-pyridine). Journal of Chemical Physics, 2001, 114, 4243-4252.	1.2	12

#	Article	IF	CITATIONS
109	Sputter-cleaned Epitaxial VxMo(1-x)Ny/MgO(001) Thin Films Analyzed by X-ray Photoelectron Spectroscopy: 1. Single-crystal V0.48Mo0.52N0.64. Surface Science Spectra, 2013, 20, 68-73.	0.3	12
110	Sputter-cleaned Epitaxial VxMo(1-x)Ny/MgO(001) Thin Films Analyzed by X-ray Photoelectron Spectroscopy: 2. Single-crystal V0.47Mo0.53N0.92. Surface Science Spectra, 2013, 20, 74-79.	0.3	11
111	Growth and properties of amorphous Ti–B–Si–N thin films deposited by hybrid HIPIMS/DC-magnetron co-sputtering from TiB2 and Si targets. Surface and Coatings Technology, 2014, 259, 442-447.	2.2	11
112	Comparative study of macro- and microtribological properties of carbon nitride thin films deposited by HiPIMS. Wear, 2017, 370-371, 1-8.	1.5	11
113	Thermally induced structural evolution and age-hardening of polycrystalline V1–xMoxN (xÂâ‰^Â0.4) thin films. Surface and Coatings Technology, 2021, 405, 126723.	2.2	11
114	Hybrid interfaces in polymer-based electronics. Synthetic Metals, 2001, 121, 1625-1628.	2.1	10
115	Photoelectron spectroscopy study of the energy level alignment at polymer/electrode interfaces in light emitting devices. Current Applied Physics, 2001, 1, 98-106.	1.1	10
116	Microstructure evolution of Ti3SiC2 compound cathodes during reactive cathodic arc evaporation. Journal of Vacuum Science and Technology A: Vacuum, Surfaces and Films, 2011, 29, 031601.	0.9	10
117	Synthesis and characterization of Zr2Al3C4 thin films. Thin Solid Films, 2015, 595, 142-147.	0.8	10
118	Native target chemistry during reactive dc magnetron sputtering studied by <i>ex-situ x</i> -ray photoelectron spectroscopy. Applied Physics Letters, 2017, 111, .	1.5	10
119	Substantial difference in target surface chemistry between reactive dc and high power impulse magnetron sputtering. Journal Physics D: Applied Physics, 2018, 51, 05LT01.	1.3	10
120	Modifications in structural, optical and electrical properties of epitaxial graphene on SiC due to 100 MeV silver ion irradiation. Materials Science in Semiconductor Processing, 2018, 74, 122-128.	1.9	10
121	A simple model for non-saturated reactive sputtering processes. Thin Solid Films, 2019, 688, 137413.	0.8	10
122	Cubic-structure Al-rich TiAlSiN thin films grown by hybrid high-power impulse magnetron co-sputtering with synchronized Al+ irradiation. Surface and Coatings Technology, 2020, 385, 125364.	2.2	10
123	Self-structuring in Zr1â^'xAlxN films as a function of composition and growth temperature. Scientific Reports, 2018, 8, 16327.	1.6	9
124	Dense Ti0.67Hf0.33B1.7 thin films grown by hybrid HfB2-HiPIMS/TiB2-DCMS co-sputtering without external heating. Vacuum, 2021, 186, 110057.	1.6	9
125	Sputter-cleaned Epitaxial VxMo(1-x)Ny/MgO(001) Thin Films Analyzed by X-ray Photoelectron Spectroscopy: 3. Polycrystalline V0.49Mo0.51N1.02. Surface Science Spectra, 2013, 20, 80-85.	0.3	8
126	Compositional dependence of epitaxial Tin+1SiCn MAX-phase thin films grown from a Ti3SiC2 compound target. Journal of Vacuum Science and Technology A: Vacuum, Surfaces and Films, 2019, 37, .	0.9	8

#	Article	IF	CITATIONS
127	Cobalt thin films as water-recombination electrocatalysts. Surface and Coatings Technology, 2020, 404, 126643.	2.2	8
128	Dense, single-phase, hard, and stress-free Ti0.32Al0.63W0.05N films grown by magnetron sputtering with dramatically reduced energy consumption. Scientific Reports, 2022, 12, 2166.	1.6	8
129	Undressing the myth of apparent constant binding energy of the C 1 s peak from adventitious carbon in x-ray photoelectron spectroscopy. , 2022, 1, 100007.		8
130	High-entropy transition metal nitride thin films alloyed with Al: Microstructure, phase composition and mechanical properties. Materials and Design, 2022, 219, 110798.	3.3	8
131	Photoelectron spectroscopy of hybrid interfaces for light emitting diodes: Influence of the substrate work function. Applied Physics Letters, 2001, 79, 3185-3187.	1.5	7
132	Novel hard, tough HfAlSiN multilayers, defined by alternating Si bond structure, deposited using modulated high-flux, low-energy ion irradiation of the growing film. Journal of Vacuum Science and Technology A: Vacuum, Surfaces and Films, 2015, 33, .	0.9	7
133	Quasi-amorphous, nanostructural CoCrMoC/a-C:H coatings deposited by reactive magnetron sputtering. Surface and Coatings Technology, 2019, 378, 124910.	2.2	7
134	Structural Modifications in Epitaxial Graphene on SiC Following 10 keV Nitrogen Ion Implantation. Applied Sciences (Switzerland), 2020, 10, 4013.	1.3	7
135	X-ray photoelectron spectroscopy analysis of TiBx (1.3 â‰â€‰x â‰â€‰3.0) thin films. Journal of Vac and Technology A: Vacuum, Surfaces and Films, 2021, 39, .	:uum Scier	nce
136	Reactive magnetron sputtering of tungsten target in krypton/trimethylboron atmosphere. Thin Solid Films, 2019, 688, 137384.	0.8	6
137	Thermal, electrical, and mechanical properties of hard nitrogen-alloyed Cr thin films deposited by magnetron sputtering. Surface and Coatings Technology, 2022, 441, 128575.	2.2	6
138	Corrosion Resistant TiTaN and TiTaAlN Thin Films Grown by Hybrid HiPIMS/DCMS Using Synchronized Pulsed Substrate Bias with No External Substrate Heating. Coatings, 2019, 9, 841.	1.2	5
139	Orthorhombic Ta3-xN5-yOy thin films grown by unbalanced magnetron sputtering: The role of oxygen on structure, composition, and optical properties. Surface and Coatings Technology, 2021, 406, 126665.	2.2	5
140	Phase formation and structural evolution of multicomponent (CrFeCo)1-yNy films. Surface and Coatings Technology, 2021, 412, 127059.	2.2	5
141	Structural and mechanical properties of amorphous AlMgB14 thin films deposited by DC magnetron sputtering on Si, Al2O3 and MgO substrates. Applied Physics A: Materials Science and Processing, 2020, 126, 1.	1.1	5
142	Preparation and tunable optical properties of amorphous AlSiO thin films. Vacuum, 2021, 187, 110074.	1.6	4
143	Improving oxidation and wear resistance of TiB2 films by nano-multilayering with Cr. Surface and Coatings Technology, 2022, 436, 128337.	2.2	4
144	Domain epitaxial growth of Ta3N5 film on c-plane sapphire substrate. Surface and Coatings Technology, 2022, 443, 128581.	2.2	4

#	Article	IF	CITATIONS
145	Electrical resistivity modulation of thermoelectric iron based nanocomposites. Vacuum, 2018, 157, 384-390.	1.6	3
146	Influence of Si doping and O2 flow on arc-deposited (Al,Cr)2O3 coatings. Journal of Vacuum Science and Technology A: Vacuum, Surfaces and Films, 2019, 37, 061516.	0.9	3
147	Microstructure, mechanical, and corrosion properties of Zr1-xCrxBy diboride alloy thin films grown by hybrid high power impulse/DC magnetron co-sputtering. Applied Surface Science, 2022, 591, 153164.	3.1	3
148	Phase Transformation and Superstructure Formation in (Ti0.5, Mg0.5)N Thin Films through High-Temperature Annealing. Coatings, 2021, 11, 89.	1.2	2
149	Study of Cucurbit[7]uril nanocoating on epitaxial graphene to design a versatile sensing platform. Applied Surface Science, 2021, 563, 150096.	3.1	2
150	Nano-columnar, self-organised NiCrC/a-C:H thin films deposited by magnetron sputtering. Applied Surface Science, 2022, 591, 153134.	3.1	2
151	Reprint of: Improving oxidation and wear resistance of TiB2 films by nano-multilayering with Cr. Surface and Coatings Technology, 2022, 442, 128602.	2.2	2
152	Energy level alignment at polymer/electrode interfaces in light-emitting devices studied by photoelectron spectroscopy. , 2001, , .		1
153	Electronic excitation of transition metal nitrides by light ions with keV energies. Journal of Physics Condensed Matter, 2020, 32, 405502.	0.7	1
154	Photoelectron Spectroscopy of Interfaces for Polymer-Based Electronic Devices. , 2001, , .		1
155	Thin Interfacial Layers in Polymer-Based Electronics. Materials Research Society Symposia Proceedings, 2000, 660, .	0.1	0
156	Thin Interfacial Layers in Polymer-Based Electronics. Materials Research Society Symposia Proceedings, 2000, 660, 1.	0.1	0
157	ICMCTF 2017 – Preface. Surface and Coatings Technology, 2017, 332, 1.	2.2	0